Stored blood has compromised oxygen unloading kinetics that can be normalized with rejuvenation and predicted from corpuscular side-scatter

Killian Donovan,[1] Athinoula Meli,[2] Francesca Cendali,[3] Kyung Chan Park[1] Rebecca Cardigan,[2,4] Simon Stanworth,[5,6,7] Stuart McKechnie,[8] Angelo D'Alessandro,[3] Peter A. Smethurst[2] and Pawel Swietach[1]

[1]Department of Physiology, Anatomy & Genetics, University of Oxford, Oxford, UK; [2]Component Development Laboratory, NHS Blood and Transplant, Cambridge, UK; [3]Department of Biochemistry and Molecular Genetics, University of Colorado Anschutz Medical Campus, Aurora, CO, USA; [4]Department of Haematology, University of Cambridge, Cambridge, UK; [5]Transfusion Medicine, NHS Blood and Transplant, Oxford, UK; [6]Department of Haematology, Oxford University Hospitals NHS Foundation Trust, Oxford, UK; [7]Radcliffe Department of Medicine, University of Oxford, and Oxford BRC Haematology Theme, Oxford, UK and [8]Adult Intensive Care Unit, John Radcliffe Hospital, Oxford University Hospitals NHS Foundation Trust, Oxford, UK

Correspondence: PAWEL SWIETACH - pawel.swietach@dpag.ox.ac.uk

doi:10.3324/haematol.2021.279296

SUPPLEMENTARY FIGURES

FIGURE S1

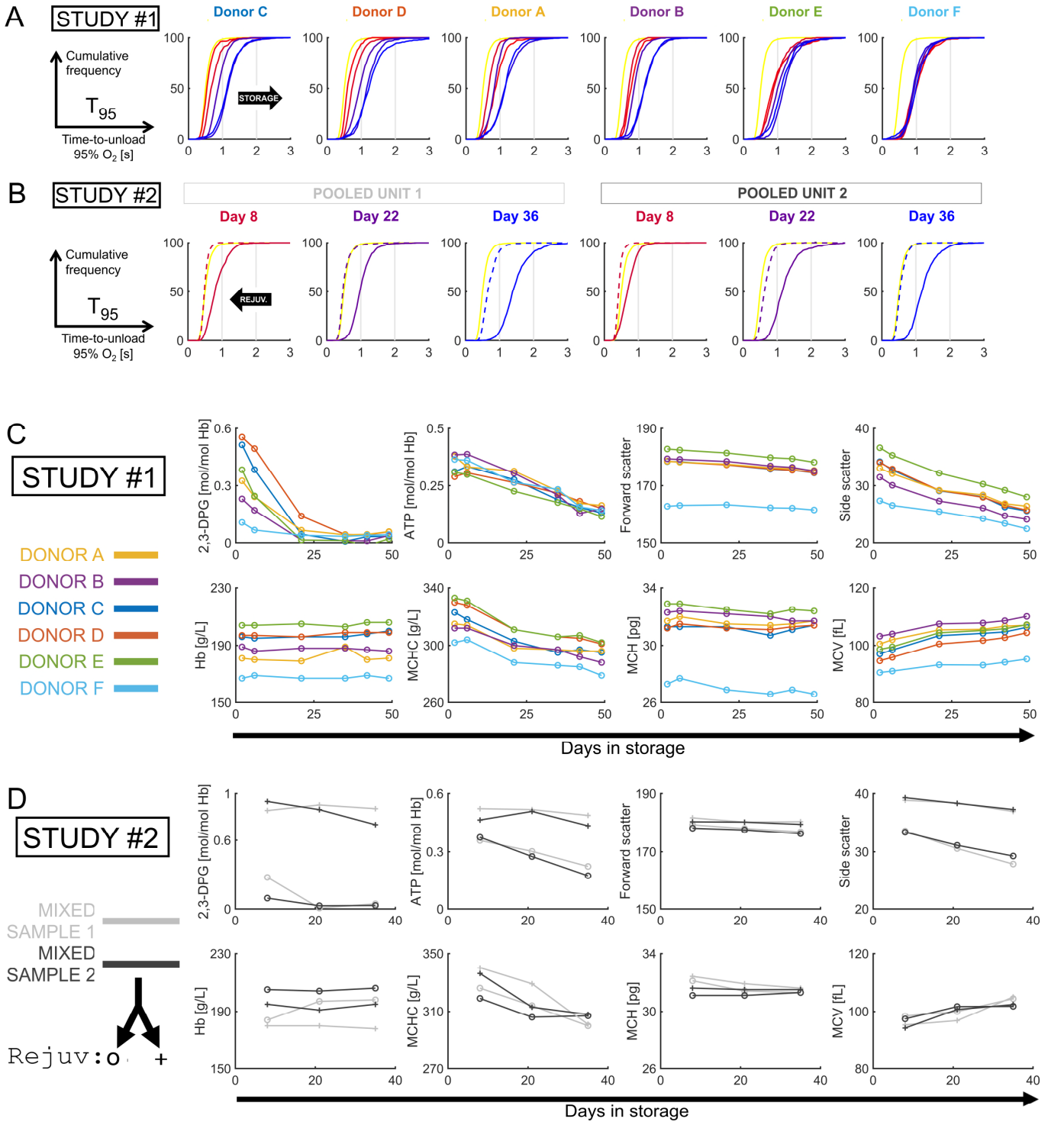

Figure S1: (A.) Mathematical transformation of τ data from Study #1 into cumulative frequency diagrams. These show the fraction of RBCs that can unload 95% of O_2 cargo in a given time T_{95}, related mathematically to τ by the equation $T_{95} = -\log(0.05)\times\tau$. To relate these kinetics to physiological conditions, T_{95} was scaled to account for temperature (0.774), the presence of CO_2 (0.949) and diffusion taking place across both sides of RBCs (0.25), as explained in Richardson *et al.* The most striking differences between RCC units occur in early storage, when some units (C, D) support near-complete gas exchange in 1 s, but others (E, F) succumb to the dysfunctional phenotype. (B.) Transformation of τ data from Study #2 into cumulative frequency diagrams for T_{95}. Rejuvenation normalizes T_{95} at all storage time-points and in both RCC pools tested. (C.) Data replotted from Figure 2A, presenting results of Study #1 separately. (D.) Data replotted from Figure 2A, presenting results of Study #2 separately.

FIGURE S2

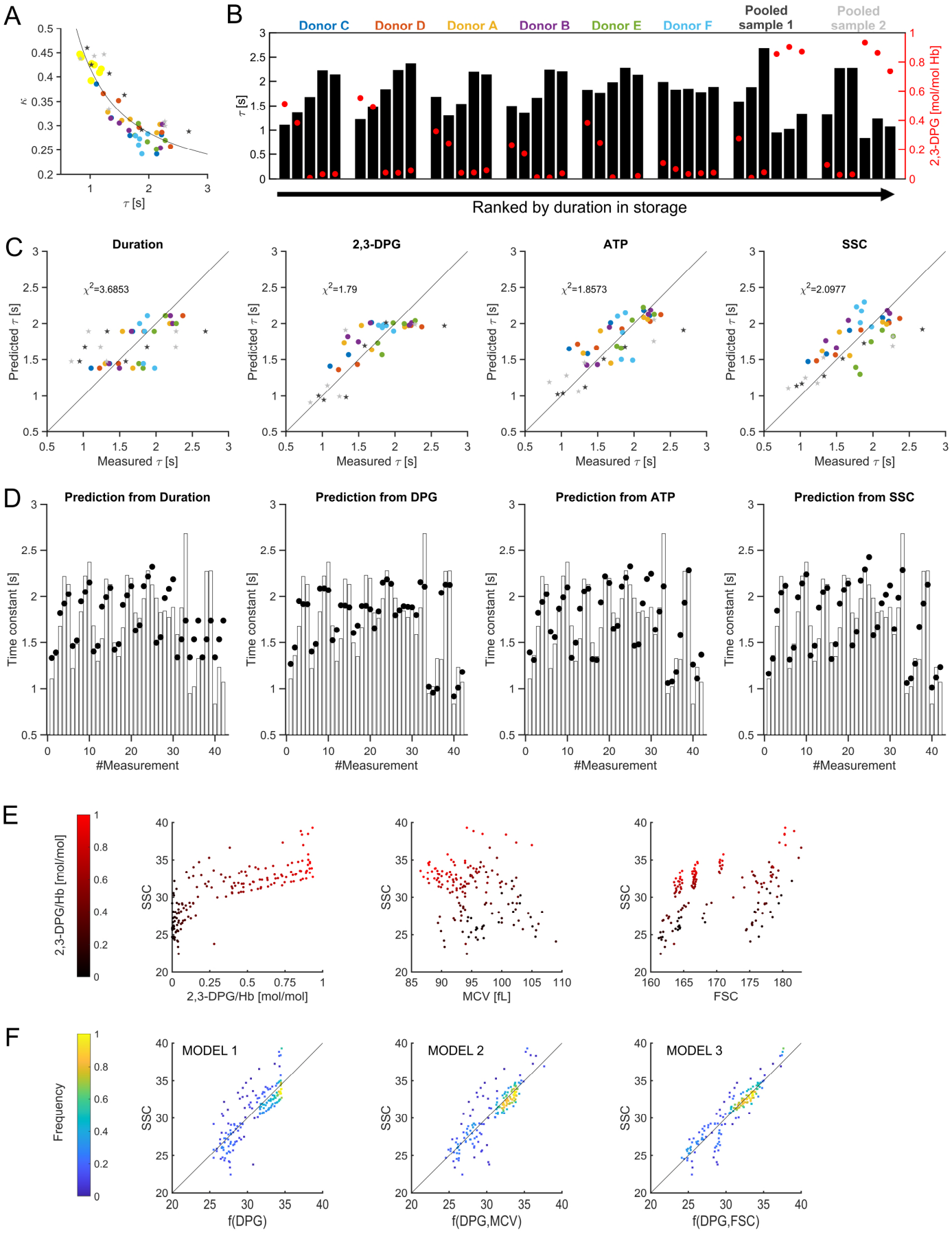

(see overleaf for legend)

Figure S2: (A.) Inverse relationship between τ and κ plotted for six RCC units, two RCC pools, and six freshly collected venous blood samples. Color coding refers to RCC unit/pool (see legend to Figure 2A); yellow datapoints refer to 6 donors providing freshly collected venous blood. Best-fit: $\kappa = 0.1528+0.2652/\tau$. (B.) 2,3-DPG levels normalized to Hb (red circles) correlate inversely with τ (black bars). However, beyond storage day 21, 2,3-DPG is depleted and loses power to predict the progression of storage-related kinetic dysfunction. (C.) Uni-variate regression analyses to determine the ability of storage duration, [2,3-DPG] normalized to Hb, [ATP] normalized to Hb, or flow-cytometric SSC to predict actual τ. In this instance, sample-level effects were not factored. Circles and stars indicate data from Study #1 and #2, respectively. Goodness-of-fit quantified by Chi-squared test; the best predictive power is achieved with SSC. (D.) Predictive power of storage duration, [2,3-DPG], [ATP], and SSC (denoted as circles) comparted to actual measurements (denoted as empty bars). In this analysis, sample-level effects were modelled with a random intercept. (E.) Relationship between SSC and the state of metabolism gauged by [2,3-DPG], and between SSC and one of two measures of corpuscular volume: MCV (derived from hematocrit) and FSC (derived from flow cytometry). Dataset of 159 measurements from 26 RCC units. (F.) Deconvoluting the components that underpin SSC using regression analysis. Relationship between SSC and [2,3-DPG] (normalized to [Hb]). Model 1 (f(DPG)=a+b×DPG^c) predicts a positive non-linear relationship between SSC and 2,3-DPG, with χ^2 of 21.3. SSC data correlated with 2,3-DPG, but the resolving power decreased once [2,3-DPG] approached zero. Model 2 (f(DPG,MCV)=a+b×DPG^c+d×MCV) includes MCV as a measure of volume. Goodness-of-fit is improved, with χ^2 of 17.2. (C.) Model 3 (f(DPG,FSC)=a+b×DPG^c+d×FSC) includes FSC as a measure of volume. Goodness-of-fit is improved further, with χ^2 of 9.9. Thus, the model that best describes SSC is a function of DPG (positive) and FSC (negative).

FIGURE S3

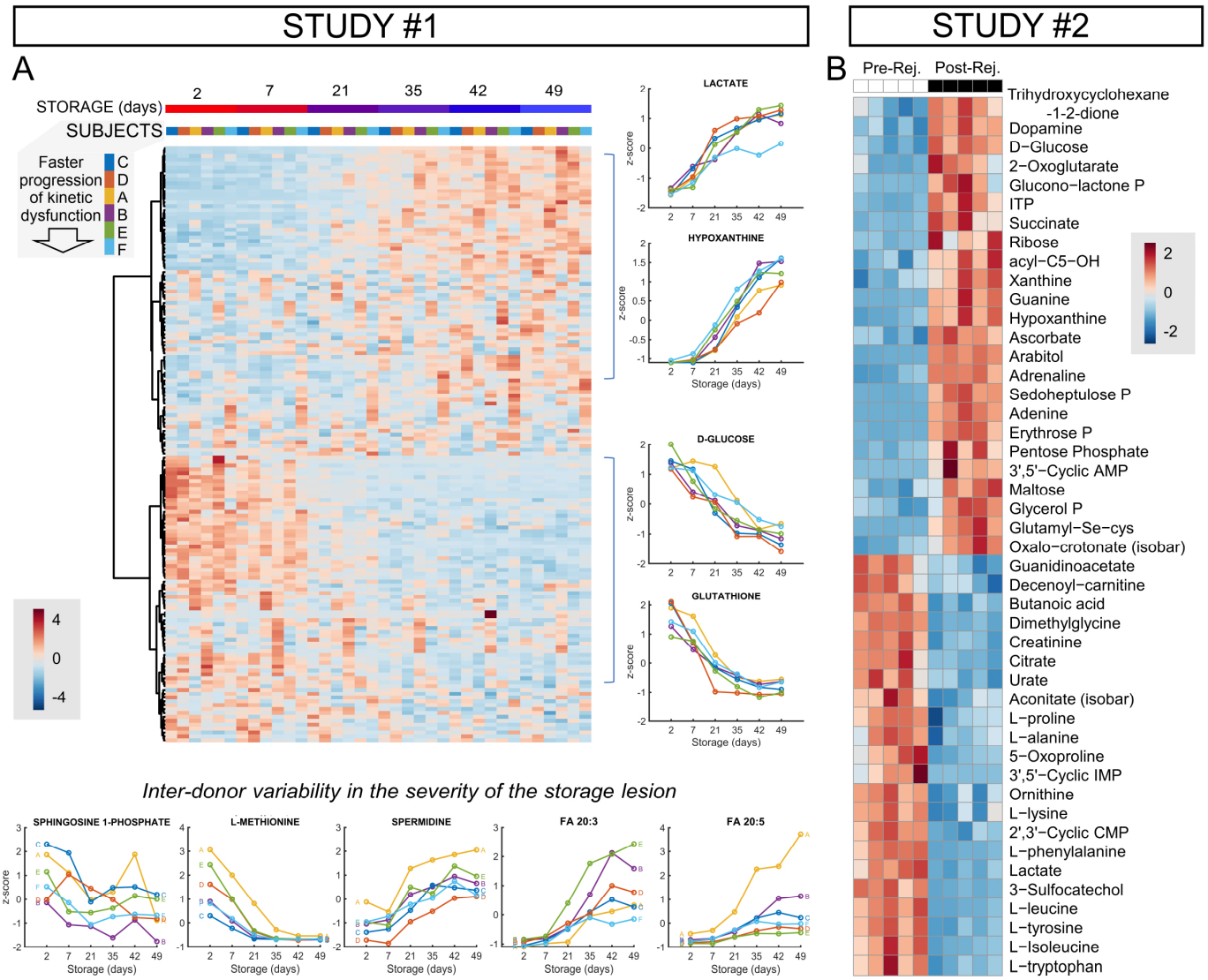

Figure S3: (A.) Hierarchical clustering analysis of metabolomics data from Study #1, using storage duration and donor units as the independent variables. Donor-specific plots aligned vertically show storage-dependent trends for four representative metabolic markers of the storage lesion: two increasing with duration (lactate, hypoxanthine) and two showing the inverse relationship (glucose, reduced glutathione). Horizontally aligned plots show metabolites affected by storage duration and a significant inter-donor variability. FA: fatty acids, including icosatrienoic (FA 20:3), arachidonic (FA 20:4) and eicosapentaenoic acid (FA 20:5). (B.) Hierarchical clustering analysis of metabolomics data from Study #2, showing the effect of rejuvenation. Among the significant hits are metabolites sensitive to changes in early and late glycolysis (lactate removal), the pentose phosphate pathway (oxidative/non-oxidative phase metabolites increased), and purine metabolism.